Physica Scripta

PAPER

Superluminality in parity-time symmetric Bragg gratings

Li-Ting Wu[1], Xin-Zhe Zhang[2], Tian-Jing Guo[3], Ming Kang[4] and Jing Chen[2,*]

[1] School of Information and Communication Engineering, Nanjing Institute of Technology, Nanjing 211167, People's Republic of China
[2] MOE Key Laboratory of Weak-Light Nonlinear Photonics and School of Physics, Nankai University, Tianjin 300071, People's Republic of China
[3] Institute of Space Science and Technology, Nanchang University, Nanchang 330031, People's Republic of China
[4] College of Physics and Materials Science, Tianjin Normal University, Tianjin 300387, People's Republic of China
[*] Author to whom any correspondence should be addressed.

E-mail: mingkang@mail.nankai.edu.cn **and** jchen4@nankai.edu.cn

Keywords: non-Hermitian optics, superluminality, parity-time symmetry

RECEIVED
9 June 2024

REVISED
3 July 2024

ACCEPTED FOR PUBLICATION
15 July 2024

PUBLISHED
24 July 2024

Abstract

Parity-time ($\mathcal{PT}$) symmetric Bragg gratings (PTBGs) possess unique features compared to traditional ones. For example, the photonic bandgap of a PTBG can be modified and even closed when the $\mathcal{PT}$ symmetry evolves from an exact phase to a broken one, and the complex reflection coefficient of a PTBG is sensitive to the direction of incidence. In this article, we reveal how the superluminal effects of transmission behave following the modified band structure of PTBGs. The superluminality of the directionally sensitive reflection is also discussed. We then investigate the Hartman effect and argue that, to account for the superluminal effects in PTBGs, a directionally sensitive dwell time should be applied. This study offers unique insights into the mechanisms of superluminality and group delay of light in non-Hermitian open systems and contributes to the advancement of PTBGs, which can eventually become an indispensable platform for probing some of the exotic properties of optical wave phenomena and light–matter interactions.

1. Introduction

The faster-than-c superluminal effect is an interesting topic of investigation because it seemingly violates Einstein's theory of special relativity and the principle of causality, which states that the speed of any signal cannot exceed the velocity of light c [1–7]. Various mechanisms of optical superluminality have been proposed and verified, including the propagation of light pulses in media with either gain-induced abnormal dispersions or negative indexes [4–6], in photonic time crystals where the refractive index oscillates periodically in time [7], and the tunneling through opaque barriers or photonic bandgaps (PBGs) [1–3].

Recent advancements of parity-time ($\mathcal{PT}$) symmetry [8–12] provide a new avenue for investigating the superluminal tunneling effect of light. Considering a traditional passive Bragg grating (i.e. one-dimensional photonic crystals) in which the real part n_r of the refractive index n varies periodically in space. In the dispersion curves of such a grating, certain PBGs emerge, which prohibit the propagation of any modes and result in strong reflection of incident fields. These properties make passive Bragg gratings valuable for constructing high-Q resonators, which serve as indispensable platforms for probing some exotic properties of optical wave phenomena and light–matter interactions. Furthermore, the tunneling process through a PBG has been shown to be superluminal, meaning that the group delay of transmission (GDT) τ_{gt} is shorter than the background group delay τ_{gb} required for traversing the same distance directly [3, 13–16]. The principle of causality is argued to be preserved in this process because the tunneling coefficient is very weak, and the signal or message is primarily held by the reflected field [13].

The presence of $\mathcal{PT}$ symmetry significantly alters the characteristics of PBGs. In $\mathcal{PT}$-symmetric Bragg gratings (PTBGs), both the real component n_r and the imaginary component n_i of the refractive index $n = n_r + jn_i$ are modulated periodically in space. The modulation periods d of n_r and n_i are equal, but their peaks are shifted by a quarter of d, rendering the structure no longer inversion symmetric (see figure 1). The

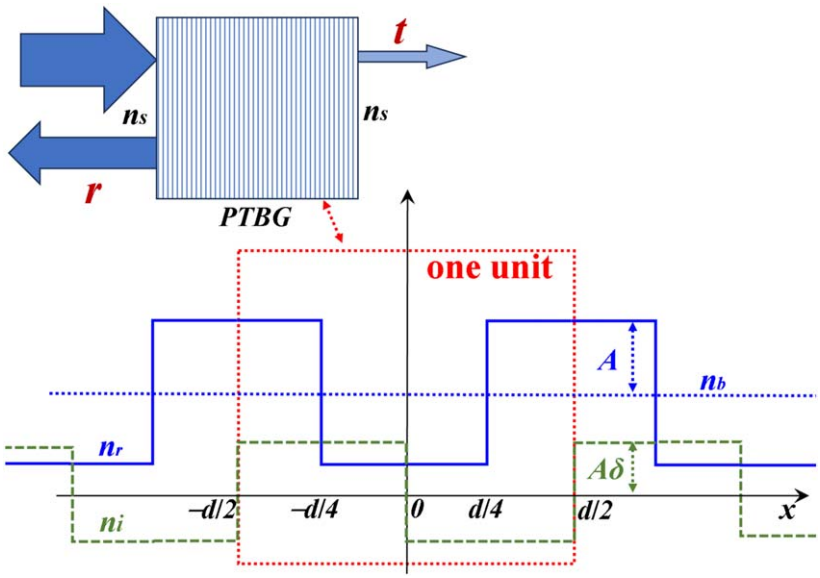

Figure 1. Schematic of the PTBG configuration under investigation. We are interested in the transmission and reflection features of the 1st PBG. Inset depicts the forward incidence.

modulation in n_i can modify the widths of PBGs and even close them when crossing exceptional points (EPs) [8–12], triggering a phase transition from the unbroken $\mathcal{PT}$ phase to the broken one [17–20]. The modified PBGs of PTBGs offer a range of interesting applications, including the realization of unidirectional invisibility [21–25], the construction of single-mode lasers [26–28], and the generation of power oscillations [29–31]. In addition, inhomogeneous [32] and nonlinear PTBGs [33, 34], along with various nonlinear effects such as bistability [35], instability [36], and solitons [37, 38], have also been investigated. As the width of a PBG dictates certain characteristics of tunneling, this article focuses on the associated superluminal effect in PTBGs. Although superluminal aspects of $\mathcal{PT}$ systems have been explored by other research groups [39–41], to the best of our knowledge, the specific topic addressed in this article has not been previously reported.

Furthermore, it has been argued that the reflection associated with tunneling through a barrier or a PBG is also superluminal (see [13] and references therein). For a symmetric barrier, the group delay of reflection (GDR) τ_{gr} equals the group delay of transmission (GDT) τ_{gt} [13]. However, PTBGs differ from ordinary ones in several aspects. For example, although gain-loss elements alone or $\mathcal{PT}$ symmetry cannot induce nonreciprocal transmission without the presence of time-reversal symmetry breaking factors such as nonlinearity, magnetic fields, or time-modulation [42–44], the magnitude of reflection from a PTBG is sensitive to the direction of incidence [8, 9, 21–26, 42–44]. The reflection coefficient of intensity from a PTBG can even exceed unity because the system is non-Hermitian and energy is not conserved within it. These features are absent in ordinary passive structures. Since the reflection from a PBG also exhibits superluminal characteristics [13], PTBGs provide an opportunity to examine and challenge many well-known conclusions about the superluminality of light and the principle of causality.

In light of the above considerations, this article focuses on the superluminal effects in PTBGs. We investigate how the delay times (τ_{gr} and τ_{gt}) vary with the adjustable PBG at different $\mathcal{PT}$ phases. The underlying physical mechanism is briefly explored using the Hartman effect [45–50] and the concept of dwell times [13]. This study aims to contribute to our understanding of the longstanding paradox of superluminality, highlight the advantages of $\mathcal{PT}$ symmetry, and advance the development of PTBGs for various important applications.

2. Method and analysis

2.1. Photonic band structure and superluminality in the exact $\mathcal{PT}$ phase

The structure of a PTBG is shown in figure 1. The growth direction of the multilayer is x, and the forward (backward) incidence represents the case that the input field comes from the left (right) and propagates toward the $+x$ ($-x$) direction. Media inside the structure are nonmagnetic, so only the dielectric constant ε varies periodically. To ensure the $\mathcal{PT}$ symmetry of $n(x) = n^*(-x)$ [8, 9], we can define the distribution of n inside a unit cell within $-0.5d < x < 0.5d$ by

$$n(x) = \begin{cases} n_b + A(1 - j\delta), & -0.5d < x < -0.25d, \\ n_b - A(1 + j\delta), & -0.25d < x < 0, \\ n_b - A(1 - j\delta), & 0 < x < 0.25d, \\ n_b + A(1 + j\delta), & 0.25d < x < 0.5d, \end{cases} \tag{1}$$

with $n(x + d) = n(x)$, d is the period. Here n_b is the background index of refraction in PTBG, A and $A\delta$ are the amplitudes of modulation in n_r and n_i, respectively. All these parameters are real. In our study we set $n_b = 1.5$ and $A = 0.1$, and change the variable δ to see how the photonic band structure, the complex coefficients of reflection and transmission, and the superluminality vary with the $\mathcal{PT}$ symmetry. Since we are interested in free-standing PTBGs, the input and output regions are assumed to be vacuum with $n_s = 1$. In experiments, the PTBG structures can also be fabricated in certain substrates, e.g. in fiber Bragg gratings with $n_s = n_b$ outside the gratings [8, 9, 22, 23, 32]. However, different choices of n_s would not modify the physics of the superluminal tunneling discussed in this article.

The optical fields inside PTBGs can be analyzed by solving the Helmholtz equation [19, 22, 28], and the modulation in n would couple the forward and backward waves together [22, 23, 33, 34]. Considering the layered configuration of PTBGs shown in figure 1, with the step-like modulations in both n_r and n_i given by equation (1), we would use the semi-analytical approach of transfer matrix method (TMM) [19, 22, 23, 28] to study the transmission/reflection spectra and the associated field distributions throughout this article. In the TMM approach, each unit of PTBG can be divided into four layers. The thickness of each layer is $d/4$, with a complex index of refraction n given by equation (1). At a given angular frequency ω, the field inside the m-th layer is expressed by a sum of forward (f) and backward (b) propagating waves, e.g. $E^{\{m\}}(x,\ t) = E_f^{\{m\}} \exp(jk_n x + j\omega t) + E_b^{\{m\}} \exp(-jk_n x + j\omega t)$ for a transverse electrical mode, where $k_n = n\omega/c$. The fields between two adjacent layers (m and $m + 1$) are related by a transfer matrix M [19, 22, 23]

$$\begin{bmatrix} E_f^{\{m+1\}} \\ E_b^{\{m+1\}} \end{bmatrix} = \begin{bmatrix} M_{11} & M_{12} \\ M_{21} & M_{22} \end{bmatrix} \begin{bmatrix} E_f^{\{m\}} \\ E_b^{\{m\}} \end{bmatrix}. \tag{2}$$

The transfer matrix M_a of the whole PTBG can be found by a sequence of matrix multiplications from the region of input to the region of output. The complex coefficients of reflection r and transmission t are rigorously defined from M_a by $r = -M_a(2, 1)/M_a(2, 2)$ and $t = M_a(1, 1) + rM_a(1, 2)$. The TMM approach can also give the dispersion of the photonic band structure. Considering the unit cell shown in figure 1, once the matrix M_u of this unit is found, the dispersion relation (ω, k) can be determined from the eigen-solutions of M_u by $\exp(-jkd) = eig(M_u)$ [19, 37], where $|k| \leqslant k_{PBG}$, $k_{PBG} = \pi/d$ is the reduced wavevector at the Brillouin zone edge.

By using TMM we first calculate the dispersion relation (ω, k) of PTBGs. The band structures at different δ values are shown in figure 2. Note that the m − th PBG is mainly formed by the coupling between the $k = \pm mk_{PBG}$ plane-wave components mediated by the Fourier component of f_m in $n(x) = n_b + \sum_{m\neq 0} f_m \exp(-j2mk_{PBG}x)$, and here we only pay attention to the 1st PBG because the magnitude of f_1 is much larger than the other components $f_{m\neq 0,1}$. Characteristics of the calculated PBG agree well with the prediction by using the plane-wave expansion (PWE) method that requires a Fourier expansion of ε^{-1} [51]. In the PWE method we need to solve the Helmholtz equation of $\varepsilon^{-1}(x)\partial^2 E_{PWE}/\partial x^2 + \omega^2 E_{PWE}/c^2 = 0$, where $E_{PWE} = \sum_m E_m \exp(-jkx - jmk_{PBG}x + j\omega t)$, m is an integer [19, 22, 28, 51]. Because the modulation in n is very weak compared to the background n_b, the lowest three components of ε^{-1} are given by $a_0 + a_+ \exp(-j2k_{PBG}x) + a_- \exp(+j2k_{PBG}x)$, where $a_0 = n_b^{-2}$, $a_+ = -2n_b^{-3}A(1 - \delta)$, and $a_- = -2n_b^{-3}A(1 + \delta)$. The first PBG is realized at the wavevector $k = k_{PBG}$, primarily consisting of $E_+ = E_0 \exp(-jk_{PBG}x + j\omega t)$ and $E_- = E_{-1} \exp(+jk_{PBG}x + j\omega t)$ within E_{PWE}, because their wavevectors have the same magnitudes and they are ω-degenerate before coupling. Only retaining these two components, and substituting ε^{-1} into the Helmholtz equation, we can find that the 1st PBG is determined by solving $[a_0,\ a_+;\ a_-,\ a_0][E_+,\ E_-]^T = (\omega/ck_{PBG})^2[E_+,\ E_-]^T$. Central point of this PBG is $\omega_{PBG} = ck_{PBG}/n_b = 2.094c/d$, and the width is $\Delta = \omega_{PBG}A\sqrt{1 - \delta^2}/n_b$. PWE predicts that an increased δ would reduce the width Δ, and an EP is achieved at $\delta = 1$ where $\Delta = 0$. When $\delta > 1$ the system should enter the broken $\mathcal{PT}$ phase [17–19].

As demonstrated in figure 2, the magnitude of δ significantly impacts the width Δ of the first PBG, in agreement with the prediction of PWE. When compared to the case with $\delta = 0$, the introduction of a non-zero δ results in a decrease in the PBG's size. When $\delta = 0.9963$ (slightly less than one because other Fourier components of ε^{-1}, though very small, still contribute to the formation of PBGs), an EP is reached. At this point, the dispersion curves exhibit linear dependence and coalesce at the band edge k_{PBG}, as shown in figure 2(c). PBG is closed in this case. With further increases in δ, the $\mathcal{PT}$ phase breaks down near the band edge. The lower (upper) branch retains a super (sub)-linear dependence, as illustrated in the zoom-in inset of figure 2(d). It is important to emphasize that the dispersion curves presented in figure 2 are obtained by scanning the solutions of $\exp(-jkd) = eig(M_u)$ [19, 37] at different real ω values. Consequently, a loop of non-zero $Im\{k\}$ within PBG

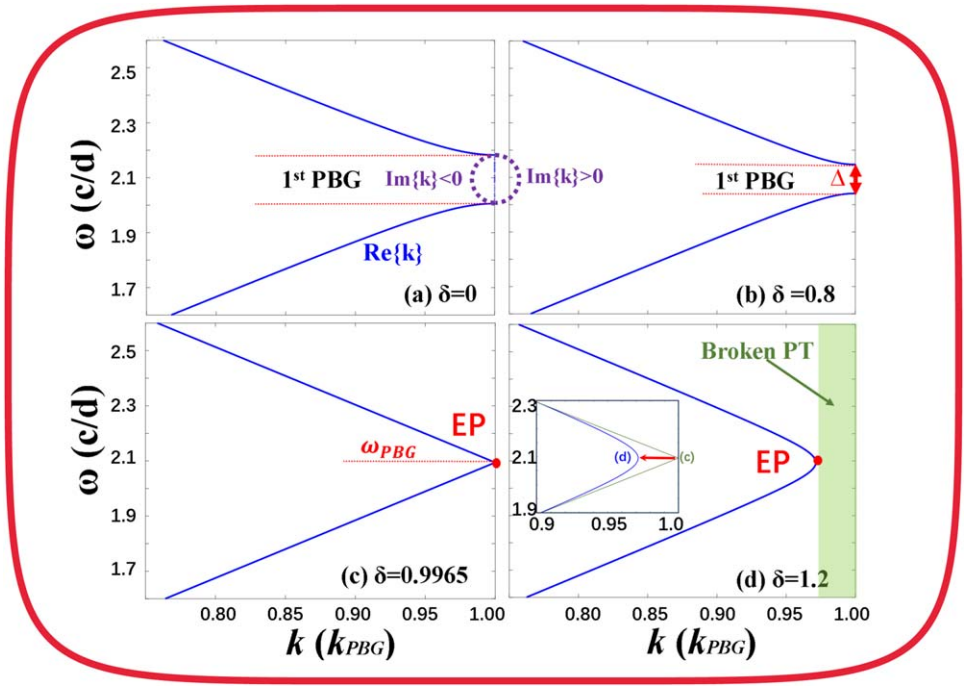

Figure 2. Dispersion curves (ω, k) of PTBGs at different δ values. Only the 1st PBG at $\omega_{PBG} = ck_{PBG}/n_b = 2.094c/d$ is displayed. (a) Inside PBG only nonzero-$Im\{k\}$ solutions (purple dashed lines) can be found. (b) when δ increases, the width Δ of PBG decreases, and finally coalesces into an EP. Inset shows a zoom-in illustration of how the dispersion curves transform from the linear dependence in (c) to the sub- or super-linear dependence in (d).

of the unbroken $\mathcal{PT}$ phase is obtained, similar to [37]. This $Im\{k\}$ loop yields two solutions at a given ω. The two solutions are opposite to each other: the one with $Im\{k\} < 0$ represents an evanescently decaying mode, while the one with $Im\{k\} > 0$ represents an evanescently growing mode [37]. In PBGs we could only excite the $Im\{k\} < 0$ mode, which plays a crucial role in the tunneling process. Furthermore, TMM cannot find the loop of non-zero $Im\{\omega\}$ in the broken $\mathcal{PT}$ phase [37], hence this loop is not depicted in figure 2(d). To identify this $Im\{\omega\}$-loop, other methods need to be employed by keeping a real value of k and scanning the complex solutions of ω, such as the one proposed in [37]. In experimental settings, real ω is always preferred and easily achievable. To experimentally access the region of non-zero $Im\{\omega\}$, state-of-the-art techniques for complex frequency waves can be utilized, as detailed in [52–54] and references therein. It's essential to remember that the band structure shown in figure 2 applies only to infinitely large structures. It is used to explain the main features in the transmission and reflection spectra, such as PBGs with $T = 0$. For finite-thickness PTBGs, the scattering of the field inevitably involves complex modes associated with the boundaries of PTBGs, which cannot be explained solely by the photonic band structure.

After analyzing the variation of PBG versus δ, we then pay attention to the transmission spectra of PTBGs. The associated transmission coefficient of intensity $T = |t|^2$ and the relative group delay Δ_t can be found by using

$$\Delta_t = \tau_{gt} - \tau_{gb}, \tag{3}$$

where $t = |t| \exp(-j\phi_t)$, the GDT τ_{gt} and the background delay τ_{gb} are defined by

$$\tau_{gt} = \frac{\partial \phi_t}{\partial \omega}, \tag{4}$$

$$\tau_{gb} = \frac{\partial (\int_{PTBG} Re\{kn_r\}\, dz)}{\partial \omega}. \tag{5}$$

When dispersion in n_b is ignored, $\tau_{gb} = n_b Nd/c$ in a N-period PTBG. Superluminality requires $\Delta_t < 0$, that τ_{gt} is shorter than the directly propagating time τ_{gb}.

Figure 3 illustrates the transmission characteristics of PTBGs with $N = 80$ for both $\delta = 0$ and $\delta = 0.8$. A region of tunneling can be observed, and its position aligns well with the 1st PBG. For instance, when $\delta = 0$, the 1st PBG falls within the angular frequency (ω) interval of 2.0072 to 2.1826 in units of c/d, and the region of $T < 0.1$ spans from 2.0043 to 2.1845. When δ increases to 0.8, the 1st PBG shifts to the range 2.004 33 to 2.1465, while the region with $T < 0.1$ now extends from 2.0385 to 2.1495. It is evident that PBG plays a crucial role in defining the tunneling region. Correspondingly, the relative group delay Δ_t also drops below zero within these

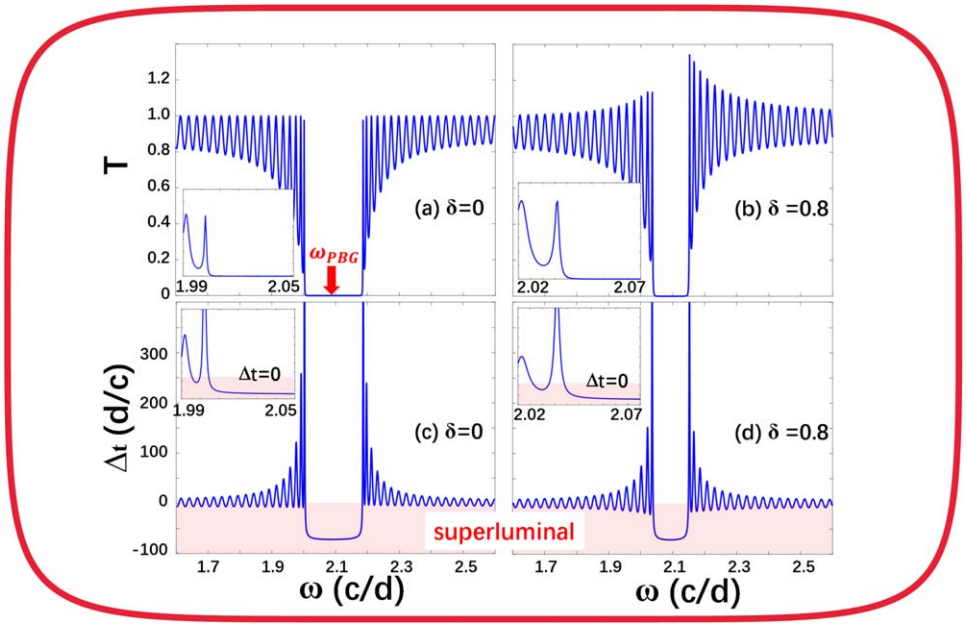

Figure 3. (a), (b) Transmission coefficient of intensity T and (c), (d) the relative group delay Δ_t when (a), (c) $\delta = 0$ (traditional Bragg grating) and (b), (d) $\delta = 0.8$ (exact $\mathcal{PT}$ phase), respectively. Here $N = 80$. The insets provide a close-up view of the curves at the long-wavelength side of PBG or tunneling region, with the y-axis limits matching those of the respective main figures.

regions, providing evidence of superluminal tunneling, as previously reported in [13]. Notably, superluminal phenomena are also observable beyond the PBG-assigned tunneling region (as shown in the insets of figure 3). However, these occurrences are relatively feeble and exhibit high vulnerability to the parameter N, in contrast to those observed within the PBG range.

2.2. Superluminality in the broken $\mathcal{PT}$ phase

With further increases in δ values, portions of the band dispersion exhibit EPs and even a broken $\mathcal{PT}$ phase, as depicted in figures 2(c) and (d). The transmission characteristics in these scenarios are investigated and presented in figure 4.

Figure 4 reveals that as we approach EP and enter the broken $\mathcal{PT}$ phase, the initial null transmission observed within PBG disappears. The value of T moves away from zero, which is directly related to the vanishing PBG of PTBGs shown in figure 2(d). Additionally, sharp transmission peaks emerge, with amplitudes that can significantly exceed unity. This indicates the presence of amplified transmission, consistent with [21–23]. Such a $T > 1$ effect can be intuitively explained by the non-Hermitian nature of PTBGs, where energy is not conserved. The incident field excites certain complex modes, whose amplitudes increase with the propagation distance x and eventually dominate the transmission.

We also investigate the relative group delay Δ_t in these scenarios and present the results in figures 4(c) and (d). Remarkably, we observe that superluminality is still achievable in the broken $\mathcal{PT}$ phase and at EP. As previously mentioned, our focus is typically on the superluminality of optical tunneling, where T is near zero, and only a very small fraction of photons survive the tunneling process through the barrier. The results displayed in figure 4 suggest that tunneling is not the only mechanism for achieving superluminality.

The significance of the results shown in figure 4 lies in their demonstration that superluminality can be observed even when the transmission efficiency is high ($T > 1$). Consequently, the superluminal effect in PTBGs is potentially easier to observe compared to traditional Bragg gratings or barriers with $T << 1$. Note that superluminality has been shown to be supported in gain media with abnormal dispersion [5, 13]. In the present study, we do not consider any abnormal dispersion in n, implying that the observed superluminality must be associated with the real wavevectors of guided modes within PTBGs. To support this claim, we can refer to the Hartman effect, which will be discussed in the next section.

Before proceeding to the next section, it is worthwhile to verify the concept of unidirectional invisibility at EP [22, 23, 32]. It is well-known that while the transmission T in a $\mathcal{PT}$ symmetric structure is independent of the direction of incidence, the reflection exhibits directional sensitivity, meaning that $R_f \neq R_b$, where f and b represent the forward and backward incidence, respectively. Unidirectional invisibility refers to the extreme wave phenomenon at EP, where $T = 1$ and either $R_f = 0$ or $R_b = 0$, but not both [22, 23, 32]. However, this effect strictly requires that the input/output regions and PTBG share the same background refractive index n_b, such as

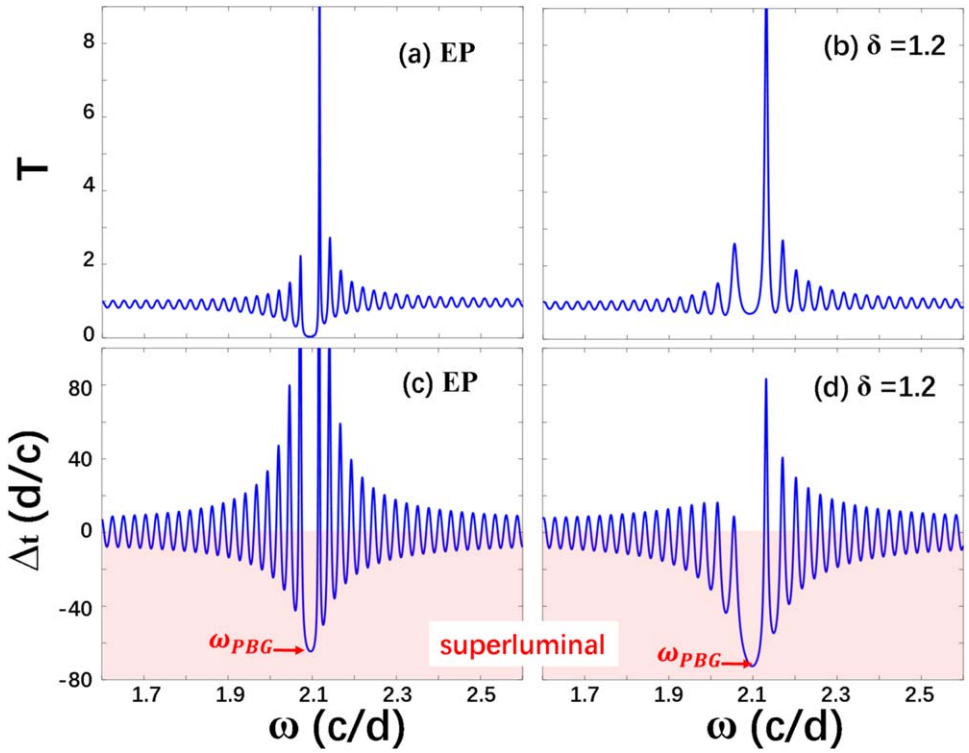

Figure 4. (a), (b) Transmission coefficient of intensity T and (c), (d) the relative group delay Δ_t when (a), (c) $\delta = 0.9963$ (EP) and (b), (d) $\delta = 1.2$ (broken $\mathcal{PT}$ phase), respectively. Here $N = 80$.

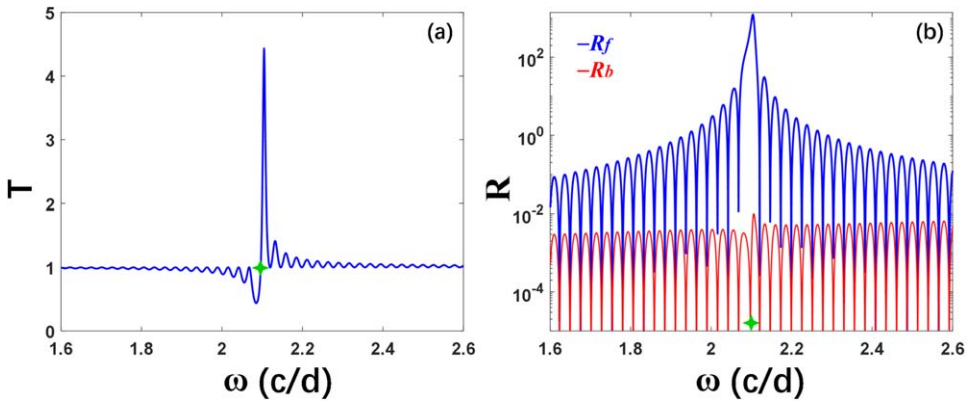

Figure 5. (a) Transmission and (b) reflection spectra of forward and backward incidences at EP. In order to observe an unidirectional invisibility at ω_{PBG}, the refractive indexes in the input and output regions are set to be $n_s = n_b = 1.5$. Note that the transmission is reciprocal so only a single curve of T is displayed in (a).

in fiber Bragg gratings [22, 23, 32]. By setting the refractive indices in the input and output regions to $n_s = n_b = 1.5$ instead of 1, we perform TMM simulations again and verify the existence of this phenomenon. Figure 5 presents the calculation results under this condition for $N = 80$. A perfect unidirectional invisibility is now achieved because $T = 1$ and R_b is nearly zero at ω_{PBG} (see green stars in figure 5).

2.3. The Hartman effect

Hartman analyzed the temporal aspects of tunneling and discovered that the delay time becomes independent of the barrier thickness and eventually saturates for very thick barriers [45–47]. The Hartman effect demonstrates that the delay in tunneling is not a transit time but a lifetime, with its origin being the saturation of stored energy when the barrier length exceeds the decay length [13]. Therefore, by utilizing the Hartman effect, we can determine which effect dominates transmission in PTBGs: the transit time of a decaying mode or the propagation of guided waves with real k.

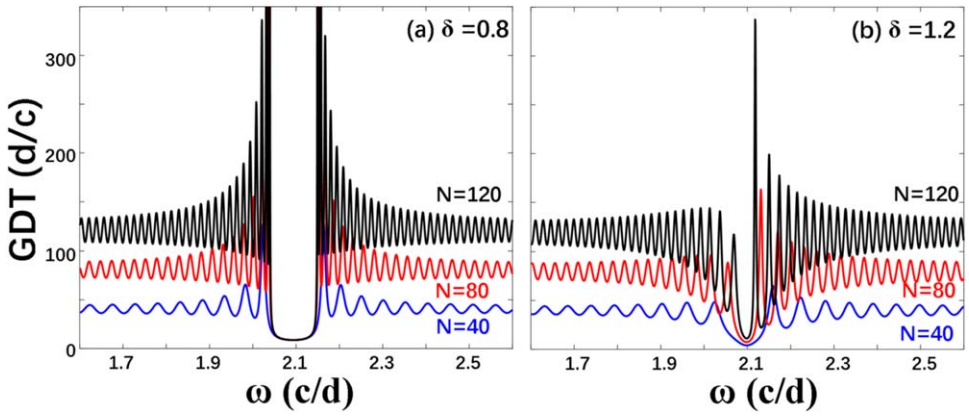

Figure 6. GDT τ_{gt} when (a) $\delta = 0.8$ where $\mathcal{PT}$ symmetry is conserved, and when (b) $\delta = 1.2$ where the $\mathcal{PT}$ phase is broken, respectively, for different numbers N of periods. Hartman effect exists only in (a).

The GDT τ_{gt} defined in equation (4) can be used to verify the Hartman effect. Figure 6 illustrates the variations of τ_{gt} versus ω at different numbers of periods N in both the unbroken ($\delta = 0.8$) and broken $\mathcal{PT}$ phase ($\delta = 1.2$). From figure 6(a), we observe that the value of τ_{gt} at ω_{PBG} remains a constant and does not change with the thickness Nd of PTBGs. The presence of the Hartman effect in figure 6(a) indicates that PTBGs now function as opaque barriers. The wavevector k of the excited mode is purely imaginary, and the field decays exponentially away from the input interface.

When the $\mathcal{PT}$ phase is broken, such as when $\delta = 1.2$ as shown in figure 6(b), the Hartman effect is no longer observed. While the τ_{gt} curve exhibits a dip at $\omega = \omega_{PBG}$, its value is no longer constant for different values of N. Considering that T is also no longer zero in this case (see figure 4), we can conclude that this dip in τ_{gt} (and in T) is not associated with a real PBG. Indeed, as indicated by the band structure in figure 2(d), the incident field at $\omega = \omega_{PBG}$ can always excite modes with non-zero $Re\{k\}$. This would preclude the Hartman effect because now the propagation effect of guided modes contributes to the transmission process.

To corroborate the above analysis, we calculate the field distributions within PTBGs. The results for the incidence of $\omega = \omega_{PBG}$ at $\delta = 0.8$ and $\delta = 1.2$ are presented in figure 7. Two different grating thicknesses, namely $N = 80$ and 120, are considered. Figures 7(a) and (c) show that when $\delta = 0.8$, where the $\mathcal{PT}$ phase is conserved, the fields inside PTBGs decay monotonically away from the input interface. Once the PTBG length Nd exceeds the decay length, any further increase in N does not alter the amplitude and pattern of the field within the structure. This demonstrates that the transmission process is analogous to the tunneling through an opaque barrier. This N-independent distribution of the evanescent field is precisely the key feature of the Hartman effect [13, 45–47].

However, a completely different scenario emerges when the $\mathcal{PT}$ phase is broken. As evident from figures 7(b) and (d), the field inside the grating is no longer evanescently decaying, and a few oscillating periods can be observed. This indicates that modes with $Re\{k\} \neq 0$ are excited. Notably, the field envelope now undergoes a long-wavelength modulation. This resembles the formation of Moire patterns through the interference among multiple modes with slightly different real wavevectors k. Unlike figures 7(a) and (c), with increased grating length Nd, the field pattern shifts along with the output interface. The maximum amplitude of the field within the structure also changes, but the period of the long-wavelength modulation remains constant. Comparing these observations to figures 7(a) and (c), the absence of the Hartman effect in this broken-$\mathcal{PT}$ phase can be readily explained, that the excited mode no longer decays purely and the transmission process primarily involves resonant propagation.

2.4. Direction-sensitive superluminal reflections

In the preceding analysis, we have demonstrated that PTBGs provide a versatile platform for manipulating and investigating the superluminal effect of optical tunneling. Now, we aim to address another crucial question: how do the superluminality manifest itself in the reflection spectra? Notably, in the study of superluminality, researchers have observed that for a symmetric barrier, the delay times in the transmission and reflection spectra are identical, meaning that $\tau_{gr} = \tau_{gt}$ [13]. However, for a PTBG, the reflection coefficient r is sensitive to the direction of incidence [8, 9], implying that this coincidence must be broken.

For this purpose we calculate the reflection coefficient of intensity $R = |r|^2$, where $r = |r| \exp(-j\phi_r)$, and the associated delay (GDR) τ_{gr} defined by

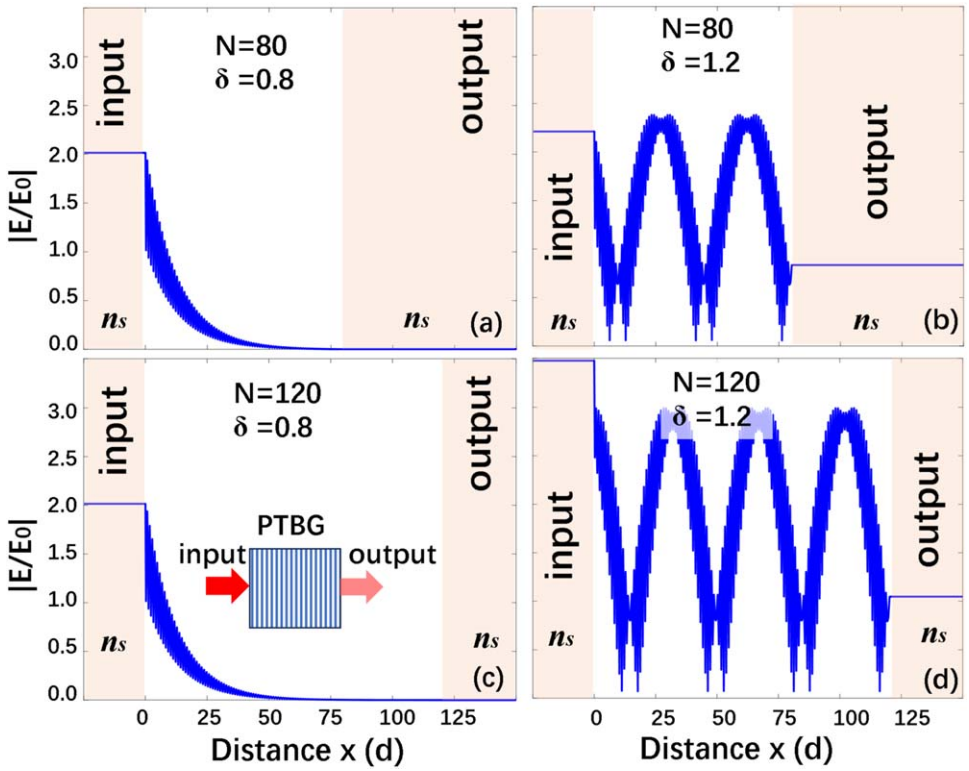

Figure 7. Distributions of field amplitude at ω_{PBG} in PTBGs for (a), (b) $N = 80$ and (c), (d) $N = 120$ and when (a), (c) $\delta = 0.8$ and (b), (d) $\delta = 1.2$, respectively. The amplitude of field E is normalized by the incident field E_i. In the input region only the reflected field E_r is displayed.

$$\tau_{gr} = \frac{\partial \phi_r}{\partial \omega}. \tag{6}$$

Results for $\delta = 0.8$ and $N = 80$ are shown in figure 8. Both forward (blue) and backward (red) incidences are calculated. For comparison, the curve of GDT τ_{gt} is also displayed alongside those of τ_{gr} as a purple line.

Consistent with the literature on directionally sensitive reflection [8, 9], we observe that R_f and R_b may have different values. Within PBG we get $R_f > R_b$. The maximum value of R_f exceeds one at ω_{PBG}, which is a non-Hermitian signature of PTBGs. Regarding GDR τ_{gr}, at ω_{PBG} all values are smaller than the background delay τ_{gb}, similar to that of GDT. Associated with the asymmetric reflection, GDR also becomes directionally dependent. GDR of the forward incidence (blue line) is smaller than that of the backward incidence (red line). In figure 8(b), we also display the curve of GDT τ_{gt}. Since transmission is independent of the direction of incidence according to the principle of reciprocity, only a single curve of GDT is shown here. From figure 8(b), we can see that τ_{gt} briefly overlaps with the forward GDR τ_{gr}.

The difference in GDR must be associated with the direction-sensitive excited field (especially the amplitude) inside PTBGs. We calculate the field distributions at ω_{PBG} for both forward and backward incidences, and show them in figures 8(c) and (d). We observe that although the decay lengths are identical in these two cases, the excited field is indeed sensitive to the direction of incidence. The amplitude of the excited field for forward incidence is larger than that for backward incidence, resulting in $R_f > R_b$.

3. Discussion

The simulations and analysis presented above confirm the existence of superluminality in both the reflection and transmission spectra of PTBGs. However, the group delay of reflection can exhibit different values for opposite incidences. The mechanism of superluminality of the directionally sensitive reflection warrants a brief discussion here.

Focusing on the scenario of conserved $\mathcal{PT}$ symmetry, Winful [13] argued that the group delay in tunneling should represent a lifetime rather than a transit time because k is purely imaginary. For electromagnetic pulses, the group delay corresponds to the lifetime of stored energy leaking out from both ends of the barrier. Since the lifetime is averaged over all incoming fields, regardless of whether they are ultimately transmitted or reflected, to be consistent with the literature [13, 48–50], the dwell time τ_d should be expressed as

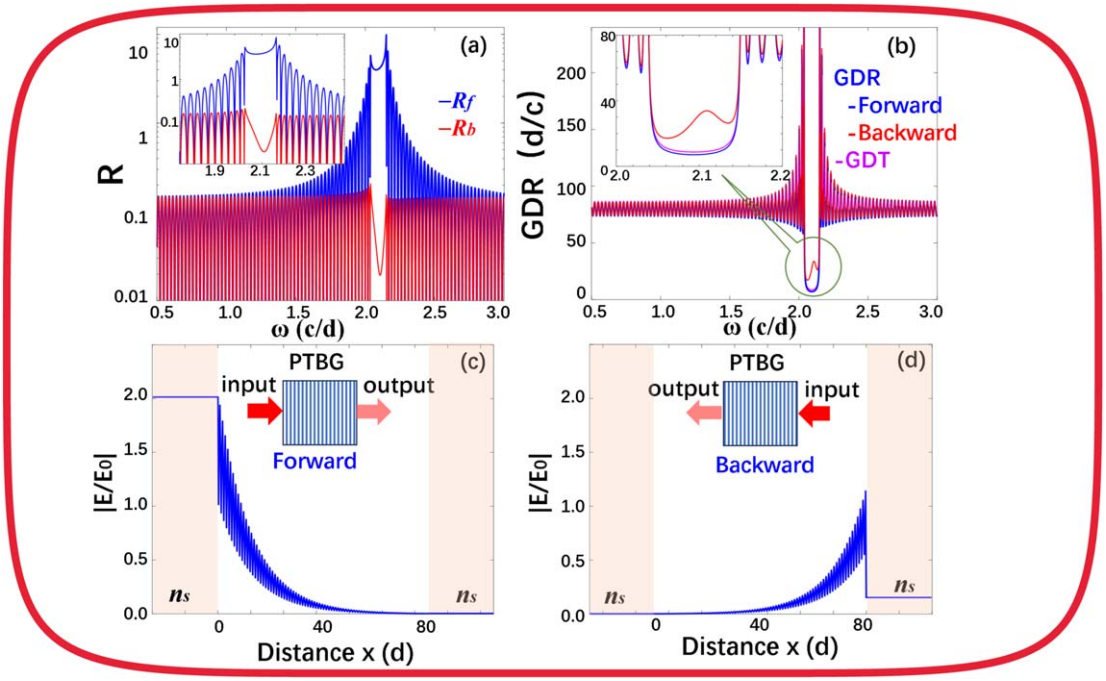

Figure 8. (a) Reflection coefficient of intensity R and (b) GDR τ_{gr} when $\delta = 0.8$. (c) and (d) are the distributions of normalized field amplitude at forward and backward incidences, respectively. In the input region only the reflected field E_r is displayed. The curve of GDT τ_{gt} is displayed in (b) as purple line. Insets are zoomed view of the curves, and the configurations of forward and backward incidences, respectively.

$$\tau_d^{-1} = \tau_{gr}^{-1} + \tau_{gt}^{-1}. \tag{7}$$

All τ_d, τ_{gr}, and τ_{gt} are positive.

Moreover, considering the standard definition of the Q-factor of a cavity and ignoring any internal loss and gain, the dwell time τ_d represents the duration required for the incident photon flux to build up the accumulated photon density or stored energy within the barrier [13]. From the different amplitudes of excited fields at opposite incidences shown in figure 8, we can infer that the dwell time should be directionally sensitive, as it would take different times to build up the different field amplitudes. Since reciprocity is still conserved in PTBGs [42–44], substituting

$$\tau_{gt}^{f} = \tau_{gt}^{b} \tag{8}$$

and the result of figure 8(b)

$$\tau_{gr}^{b} > \tau_{gr}^{f} \tag{9}$$

into equation (7), we can get

$$\tau_{d}^{b} > \tau_{d}^{f}. \tag{10}$$

This disparity in dwell times for opposite incidences is not observed in conventional photonic barriers with inversion symmetry. This observation raises intriguing questions that could be the subject of future investigations. For instance, what is the precise meaning and definition of dwell time in non-Hermitian systems (not limited to PTBGs)? Can the dwell time explain the superluminality observed in PTBGs? How can we determine or calculate the dwell time in PTBGs? Are there alternative definitions of transit or lifetime that could model the superluminality of non-Hermitian systems? We believe that addressing these open questions and proposing potential mathematical approaches should consider non-Hermitian quantum theory [40, 55–57]. Literature on non-Hermitian Hartman effects [58, 59] might also offer valuable insights. It is important to note that we have only discussed superluminal reflection at the unbroken $\mathcal{PT}$ phase. When the $\mathcal{PT}$ phase is broken, the concept of dwell time is not applicable.

In future we can also pay more attention to the superluminality at the broken $\mathcal{PT}$ phase. In subsection 2.3 we verify the Hartman effect, calculate the patterns of excited fields, and prove that the superluminality at the exact $\mathcal{PT}$ phase is indeed tunneling. Our analysis also refutes the tunneling nature of the superluminality at the broken $\mathcal{PT}$ phase. The physical mechanism behind the superluminality at the broken $\mathcal{PT}$ phase, that the superluminality persists with varied N by exciting guided modes, is beyond our current understanding and warrants further investigation in future studies.

Note that this work is theoretical, and the parameters have been chosen to simplify, condense, and illustrate our analysis. The results presented here can be applied to other harmonic waves, including but not limited to polaritons and phonons (acoustic waves). To implement our proposal experimentally, one must find ways to precisely control the spatial distributions of refractive index and gain/loss (not only their periods but also their amplitudes). Numerous important review articles [8–12, 60, 61] have explained the state-of-the-art experimental advancements in $\mathcal{PT}$ symmetry within photonic lattices, photonic crystals, and metasurfaces/metamaterials. We also note that Benisty *et al* have recently provided insights into device design rules for $\mathcal{PT}$ -symmetric gratings operating at 1550nm [62]. For more detailed information about the advancement of PTBGs in experiments, we refer readers to this literature [62] and the references therein.

Moreover, we acknowledge that experimentally observing superluminality is challenging due to the small relative advancement of a light pulse compared to its width [4, 13]. Applying similar experimental techniques to PTBGs presents additional challenges because the initially low transmission of tunneling may be further reduced, potentially causing the loss of important phase information. However, since superluminality can also be observed from the reflection spectra, whose magnitude R is much larger than T, we can focus on measuring this aspect. The superluminality of reflection also has a tangible impact on building high-Q resonators. Studying this phenomenon could enhance our understanding of the formation of resonant modes in PT resonators and drive advancements in the applications already achieved with traditional Bragg gratings.

4. Conclusion

In summary, we study how the superluminal transmission and reflection effects of PTBGs behave in both exact and broken phases of $\mathcal{PT}$ symmetry. We demonstrate that the superluminality of transmission is observable even when T is very large, while the superluminality of reflection is sensitive to the direction of incidence. Based on the Hartman effect and the distribution of fields inside PTBGs, we argue that the observed superluminality can be explained by considering three factors: the different amplitudes of excited fields inside PTBGs, the associated dwell times at opposite incidence, and the reciprocity of transmission. This study provides unique insights into the mechanisms of superluminality and group delay of light in non-Hermitian open systems. It also contributes to the advancement of PTBGs, which may eventually become an indispensable platform for probing some of the exotic properties of optical wave phenomena and light–matter interactions.

Acknowledgments

This work was supported by the Natural National Science Foundation of China (NSFC) (12104203, 12104227, 12274241), the Scientific Research Foundation of Nanjing Institute of Technology (YKJ202021), and the Jiangxi Double-Thousand Plan (No. jxsq2023101069).

Data availability statement

All data that support the findings of this study are included within the article (and any supplementary files).

ORCID iDs

Tian-Jing Guo https://orcid.org/0000-0001-8495-0051
Jing Chen https://orcid.org/0000-0001-5637-1829

References

[1] Winful H G 2003 *Phys. Rev. Lett.* **90** 023901
[2] Buttiker M and Washburn S 2003 *Nature* **422** 271
[3] Longhi S, Marano M, Laporta P and Belmonte M 2001 *Phys. Rev.* E **64** 055602
[4] Wang L J, Kuzmich A and Dogariu A 2000 *Nature* **406** 277
[5] Boyd R W and Gauthier D J 2009 *Science* **326** 1074
[6] Bashir A I, Batool S U, Arif A and Shazad A 2023 *Phys. Scr.* **98** 115116
[7] Pan Y, Cohen M I and Segev M 2023 *Phys. Rev. Lett.* **130** 233801
[8] Feng L, El-Ganainy R and Ge L 2017 *Nat. Photo.* **11** 752
[9] El-Ganainy R, Makris K G, Khajavikhan M, Musslimani Z H, Rotter S and Christodoulides D N 2018 *Nat. Phys.* **14** 11
[10] Cao H and Wiersig J 2015 *Rev. Mod. Phys.* **87** 61
[11] Ozdemir S K, Rotter S, Nori F and Yang L 2019 *Nat. Mater.* **18** 783
[12] Miri M A and Alù A 2019 *Science* **363** 42

[13] Winful H G 2006 *Phys. Rep.* **436** 1
[14] D'Aguanno G, Centini M, Scalora M, Sibilia C, Bloemer M J, Borden C M, Haus J W and Bertolotti M 2001 *Phys. Rev.* E **63** 036610
[15] Steinberg A M and Chiao R Y 1995 *Phys. Rev.* A **51** 3525
[16] Spielmann Ch, Szipocs R, Stingl A and Krausz F 1994 *Phys. Rev. Lett.* **73** 2308
[17] Makris K G, El-Ganainy R, Christodoulides D N and Musslimani Z H 2008 *Phys. Rev. Lett.* **100** 103904
[18] Zheng M C, Christodoulides D N, Fleischmann R and Kottos T 2010 *Phys. Rev.* A **82** 010103
[19] Ding K, Zhang Z Q and Chan C T 2015 *Phys. Rev.* B **92** 235310
[20] Zhang X Z, Wu L T, Luo R Z and Chen J 2023 *Phys. Scr.* **98** 095511
[21] Longhi S 2010 *Phys. Rev.* A **81** 022102
[22] Lin Z, Ramezani H, Eichelkraut T, Kottos T, Cao H and Christodoulides D N 2011 *Phys. Rev. Lett.* **106** 213901
[23] Mostafazadeh A 2013 *Phys. Rev.* A **87** 012103
[24] Keshmarzi E K, Tait R N and Berini P 2016 *Appl. Phys.* A **122** 279
[25] Lazo E and Humire F R 2023 *Phys. Scr.* **98** 035028
[26] Peng R, Li Y and Huang W 2018 *J. Light. Tech.* **36** 4074
[27] Hao T and Berini P 2022 *Opt. Express* **30** 5167
[28] Huang C Y, Zhang R, Han J L, Zheng J and Xu J Q 2014 *Phys. Rev.* A **89** 023842
[29] Brandao P A and Cavalcanti S B 2017 *Phys. Rev.* A **96** 053841
[30] Boucher Y G and Feron P 2019 *IEEE J Quan. Elect.* **55** 6000209
[31] Chen Z J, Wang H D, Luo B and Guo H 2014 *Opt. Express* **22** 25120
[32] Vignesh Raja S, Govindarajan A, Mahalingam A and Lakshmanan M 2020 *Phys. Rev.* A **101** 033814
[33] Xu Y L, Feng L, Lu M H and Chen Y F 2014 *IEEE Photonics J.* **6** 0600507
[34] Vignesh Raja S, Govindarajan A, Mahalingam A and Lakshmanan M 2019 *Phys. Rev.* A **100** 053806
[35] Phang S, Vukovic A, Susanto H, Benson T M and Sewell P 2014 *Opt. Lett.* **39** 2603
[36] Sarma A K 2014 *JOSAB* **31** 1861
[37] Ali Miri M, Aceves A B, Kottos T, Kovanis V and Christodoulides D N 2012 *Phys. Rev.* A **86** 033801
[38] Gupta S K and Sarma A K 2014 *Europhys. Lett.* **105** 44001
[39] Szameit A, Rechtsman M C, Bahat-Treidel O and Segev M 2011 *Phys. Rev.* A **84** 021806
[40] Lee Y C, Hsieh M H, Flammia S T and Lee R K 2014 *Phys. Rev. Lett.* **112** 130404
[41] Bender C M, Brody D C, Jones H F and Meister B K 2007 *Phys. Rev. Lett.* **98** 040403
[42] Peng B, Ozdemir S K, Liertzer M and Yang L 2016 *PNAS* **113** 6845
[43] Caloz C, Alu A, Tretyakov S, Sounas D, Achouri K and Deck-Leger Z-L 2018 *Phys. Rev. Appl.* **10** 047001
[44] Guo C and Fan S 2022 *Phys. Rev. Lett.* **128** 256101
[45] Hartman T E 1962 *J. Appl. Phys.* **33** 3427
[46] Olkhovsky V S and Recami E 1992 *Phys. Rep.* **214** 339
[47] Winful H G 2002 *Opt. Express* **10** 1491
[48] Buttiker M 1983 *Phys. Rev.* B **27** 6178
[49] Leavens C R and Aers G C 1989 *Phys. Rev.* B **39** 1202
[50] Buttiker M and Landauer R 1982 *Phys. Rev. Lett.* **49** 1739
[51] Zhang W, Hu A, Lei X, Xu N and Ming N 1996 *Phys. Rev.* B **54** 10280
[52] Archambault A, Besbes M and Greffet J J 2012 *Phys. Rev. Lett.* **109** 097405
[53] Guan F, Guo X, Zeng K, Zhang S, Nie Z, Ma S, Dai Q, Pendry J, Zhang X and Zhang S 2023 *Science* **381** 766
[54] Kim S, Peng Y, Yves S and Alu A 2023 *Phys. Rev.* X **13** 041024
[55] Guo P, Gasparian V, Jodar E and Wisehart C 2023 *Phys. Rev.* A **107** 032210
[56] Scheuer J 2018 *Opt. Express* **26** 32091
[57] Moiseyev N 2011 *Non-Hermitian Quantum Mechanics* (Cambridge University Press)
[58] Hasan M, Singh V N and Mandal B P 2020 *Eur. Phys. J. Plus* **135** 640
[59] Longhi S 2022 *Ann. Phys.* **534** 2200250
[60] Yan Q, Zhao B, Zhou R, Ma R, Lyu Q, Chu S, Hu X and Gong Q 2023 *Nanophotonics* **12** 2247
[61] Wang Q and Chong Y D 2023 *JOSAB* **40** 1443
[62] Benisty H, de la Perriere V B, Ramdane A and Lupu A 2021 *JOSAB* **38** c168